International Journal of Advanced and Applied Sciences, 11(1) 2024, Pages: 68-77

Contents lists available at Science-Gate

International Journal of Advanced and Applied Sciences

Journal homepage: http://www.science-gate.com/IJAAS.html

The Newtonian heating effect on MHD free convective boundary layer flow of magnetic nanofluids past a moving inclined plate

Noor Hafizah Zainal Aznam [1], Fazillah Bosli [1,*], Mohd Rijal Ilias [2], Siti Shuhada Ishak [2], Anis Mardiana Ahmad [1], Asmahani Nayan [1]

[1]*Mathematical Sciences Studies, College of Computing, Informatics, and Media, Universiti Teknologi MARA (UiTM), Kedah Branch, Sungai Petani Campus, 08400 Merbok, Kedah Darulaman, Malaysia*
[2]*School of Mathematical Sciences, College of Computing, Informatics, and Media, Universiti Teknologi MARA, 40450 Shah Alam, Selangor, Malaysia*

ARTICLE INFO

Article history:
Received 18 June 2021
Received in revised form
11 June 2023
Accepted 24 December 2023

Keywords:
Nanofluids
Free convection
MHD
Moving inclined plate
Newtonian heating

ABSTRACT

The effect of magnetic strength on the MHD free convection flow of nanofluids over a moving inclined plate with Newtonian heating is analyzed. The governing partial differential equations with Newtonian heating boundary conditions are transformed into a system of nonlinear coupled ordinary differential equations (ODEs) by using similarity transformations. The Keller Box method was used as a solvation method for ODEs. The skin friction and Nusselt number are evaluated analytically as well as numerically in a tabular form. Numerical results for velocity and temperature are shown graphically for various parameters of interest, and the physics of the problem is well explored. The significant findings of this study are promoting an angle of an aligned magnetic field, magnetic strength parameter, the angle of inclination parameter, local Grashof number, the volume fraction of nanoparticles, and Newtonian heating parameter. The result shows that the moving inclined plate in the same direction increases the skin friction coefficient and reduces the Nusselt number. It is also observed that the velocity of moving an inclined plate with the flow is higher compared to the velocity of moving an inclined plate against the flow. The temperature of a moving inclined plate with the flow is decreased much quicker than the temperature of a moving inclined plate against the flow. The other noteworthy observation of this study demonstrates that the Nusselt number in the Newtonian heating parameter shows that Fe_3O_4-kerosene is better than Fe_3O_4-water.

1. Introduction

Over the last two decades, theoretical research on the dynamics and heat transfer characteristics of nanofluids has increased tremendously. Recently, the study of nanotechnology based on nanofluids has received broad attention due to its wide-ranging applications in various engineering's and technologies. Nanofluids are potential heat transfer fluids with enhanced thermophysical characteristics and heat transfer presentation applicable in many applications for improved performances. The term nanofluid was first proposed by Choi and Eastman (1995) to describe a colloidal suspension with nanoparticles dispersed uniformly in a base fluid. Since then, rapid development related to nanofluids has been seen in many research papers that have been published. Heat transfer enhancement of nanofluids has been studied by Xuan and Li (2000), and they both further investigated the convective heat transfer and flow features of nanofluids. Moreover, Wen and Ding (2004) did an experimental investigation into the convective heat transfer of nanofluids under laminar flow conditions, while Prasher et al. (2006) measured the viscosity of the nanofluids and explored the nanofluids implication in thermal applications. A review and comparison of nanofluids' thermal conductivity and heat transfer enhancements have been reported by Yu et al. (2008). Improvement of the heat transfer in electronic cooling, heat exchangers, double plane windows, etc., is a tremendously important topic from the energy-saving point of view. Heat transfer analysis and fluid flow characteristics based on the

* Corresponding Author.
Email Address: fazillah@uitm.edu.my (F. Bosli)
https://doi.org/10.21833/ijaas.2024.01.008
Corresponding author's ORCID profile:
https://orcid.org/0009-0008-8988-4856

Tiwari-Das model were examined by Sreedevi et al. (2021) and Reddy and Sreedevi (2021) for different effects and parameters. Magnetohydrodynamic (MHD) is the study of magnetic properties and the behavior of the electrically conducting fluid. In recent years, research on the topic of MHD has developed quickly by considering the different problems and situations (Ilias et al., 2016; 2017a; 2018; 2020). The magnetic field influences on flow and heat transfer have received the attention of researchers due to potential application in real-world problems. Magnetic nanofluids in this study are represented by ferrofluids, a liquid that becomes strongly magnetized in the presence of a magnetic field. Ferrofluids can be found in many potential fields, such as medicine, aerospace, science, and engineering. As pointed out by others, research on ferrofluids was initiated by Blums (2002), who investigated the heat and mass transfer behavior. Several advanced studies have addressed the ferrofluids heat transfer (Bozhko and Putin, 2003; Ganguly et al., 2004; Jue, 2006; Arulmurugan et al., 2006). The fluid flow and heat transfer in the presence of the magnetic field by Noranuar et al. (2021) found that the temperature increases while the nanofluid velocity reduces with a higher magnetic strength. In the year 2022, the study of the nanofluids with the presence of MHD effect by Rosaidi et al. (2022), Nayan et al. (2022), Bosli et al. (2022), and Ishak et al. (2022) found that with the effect of the magnetic field increase the heat transfer as well as the velocity of the study. Study on the MHD effect was discovered in different situations by some researchers such as Ilias (2018), Ahmad et al. (2019), Khashi'ie et al. (2019), and Soid et al. (2022).

Furthermore, an experiment of enhanced ferrofluid heat transfer under the influence of a magnetic field has been done by Lajvardi et al. (2010). Sheikholeslami and Rashidi (2015) found that the Nusselt number increases by analyzing ferrofluid heat transfer in the presence of the magnetic field. The flow of magnetic nanofluid over moving inclined surfaces occurs in many physical phenomena. Its importance can be seen in fluid where heat transfer is present. In the study of fluid flow over heated surfaces, the buoyancy forces exert a strong influence on the free convection flow field in the presence of a magnetic field. Ilias et al. (2017b) studied the influence of aligned and transverse magnetic fields on the two-dimensional natural convection boundary layer flow of a ferrofluid over a fixed vertical plate in the presence of convective boundary conditions. Two different base fluids (water and kerosene) containing magnetite (Fe_3O_4) as ferroparticles are considered. They found that the heat transfer rate at the plate surface with Fe_3O_4–kerosene ferrofluid is higher than Fe_3O_4–water. The industrial and technical applications of such problems include nuclear reactors cooled during an emergency shutdown, electronic devices cooled by fans, solar central receivers exposed to wind currents, and heat exchangers placed in a low-velocity environment.

The study based on free convection fluids by most researchers is because it is easier to analyze the behavior of magnetic nanofluids because it occurs naturally and without being influenced by external forces. Ilias et al. (2020) investigated unsteady aligned MHD boundary layer flow and heat transfer of magnetic nanofluids. They discovered that the free convection parameter known as the Grashof number increases the velocity as well as the heat transfer of their study. Rosaidi et al. (2022) investigated the behavior of MHD-free convection flow of magnetic nanofluids. The study found that the Grashof number has improved the velocity field and lowered the momentum boundary layer thickness. The study on free convection was rapidly established by considering the different problems and situations by Hamdan et al. (2020) and Mohamad et al. (2022). They found that the Grashof number has a significant impact on the velocity and momentum boundary layer thickness.

Newtonian heating has been widely applied in many types of research instead of constant surface temperature because of the failure of the constant temperature assumption adapted to physical situations. Newtonian heating is defined as the process of accentuating the surface resistance and desertion of internal resistance. Heat exchanger, conjugate heat transfers around fins, and the cooling mechanism for nuclear reactors are among the application that involves Newtonian heating in their processes. Four types of temperature distributions at the wall have been studied by Merkin (1994), and one of the temperature distributions is Newtonian heating. Studies on Newtonian heating have been conducted by many researchers, such as Singh and Makinde (2012). They investigated the presence of Newtonian heating in volumetric heat of MHD-free convection flow along with the inclined plate. At the same time, Uddin et al. (2012) studied the MHD free convective boundary layer flow of a nanofluid past a vertical plate with Newtonian heating. On the bright side, the research on Newtonian heating is still ongoing. For instance, Makinde (2013) analyzed the effects of viscous dissipation and Newtonian heating on the boundary layer flow of nanofluids over a flat plate, while Hayat et al. (2017) examined the Newtonian heating effect in nanofluids flow by a permeable cylinder. Apart from that, Ullah et al. (2017) investigated the effects of slip conditions and Newtonian heating on the MHD flow of Casson fluid over a nonlinearly stretching sheet saturated in a porous medium. Recently, Mohamed et al. (2019) investigated MHD slip flow and heat transfer on the stagnation point of a magnetite ferrofluid towards a stretching sheet with Newtonian heating. They found that the magnetite ferrofluid provided higher wall temperature and heat transfer capabilities compared to water. Yasin et al. (2019) studied the MHD stagnation flow in ferrofluid over a flat plate with Newtonian heating. The study found that the velocity is increased as well as the heat transfer in magnetic parameter. Aleem et al. (2020) investigated the MHD influence on different water-based nanofluids in a porous medium with chemical reactions and Newtonian heating. They discovered that Ag-water nanofluid has a greater temperature due to its greater thermal conductivity value compared to others.

The study of the influence of magnetic field strength and Newtonian heating effects on nanofluid over the moving inclined plate has not been reported yet. The resulting governing equations are solved numerically using the Keller Box method for non-dimensional velocity and temperature profiles of the stationary inclined plate. Ilias (2018) studied the heat transfer rate of an MHD flow with a free convection effect by solving it by using the Keller box method. The study found that, for both unsteady and steady fluid flow cases, increasing nanoparticle volume fraction and magnetic field strength increase the Nusselt number. Further, the velocity and temperature profiles for moving the inclined plate with the flow and moving the inclined plate against the flow with the strength of the magnetic field are presented graphically.

2. Mathematical formulation

The steady two-dimensional, incompressible, laminar, hydromagnetic free convection of magnetic nanofluids flow with heat transfer over an inclined plate with the aligned and transverse magnetic field is considered. The plate is inclined at an angle of inclination γ measured in the clockwise direction and situated in an otherwise quiescent ambient fluid at temperature T_∞. The gravitational acceleration g is acting downward. The physical coordinates (x, y) are chosen such that $x-$axis is measured along the plate, and the $y-$axis is measured normal to the surface of the plate, as shown in Fig. 1. Water and kerosene are used as the base fluids with magnetite (Fe_3O_4) as a nanoparticle. The base fluids and nanoparticles are in thermal equilibrium, and no-slip occurs between them. The spherical-shaped nanoparticles are considered. The viscous dissipation and radiation are ignored in the analysis.

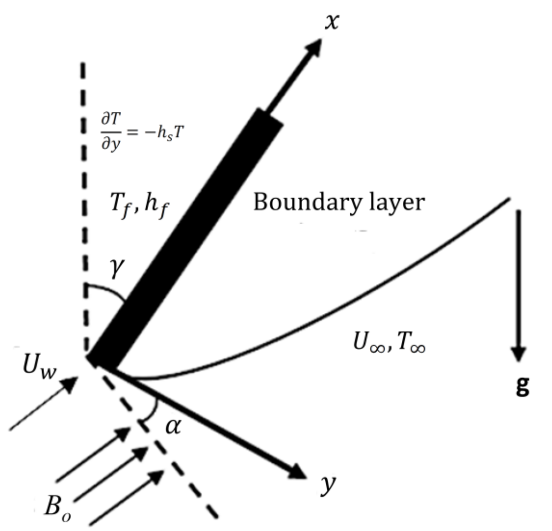

Fig. 1: Geometry of physical model

Under the above assumptions and following Tiwari and Das (2007), the equations of MHD boundary layer flow are:

$$\frac{\partial u}{\partial x} + \frac{\partial v}{\partial y} = 0 \tag{1}$$

$$u\frac{\partial u}{\partial x} + v\frac{\partial u}{\partial y} = \frac{\mu_{nf}}{\rho_{nf}}\frac{\partial^2 u}{\partial y^2} + \frac{(\rho\beta)_{nf}}{\rho_{nf}} g \cos\gamma\,(T - T_\infty) - \frac{\sigma B^2(x)}{\rho_{nf}} sin^2\alpha(u - U_\infty) \tag{2}$$

$$u\frac{\partial T}{\partial x} + v\frac{\partial T}{\partial y} = \alpha_{nf}\frac{\partial^2 T}{\partial y^2} \tag{3}$$

The boundary conditions for the velocity and temperature of this problem are given by,

$$u(x,0) = U(x) = \lambda U_\infty, \quad v(x,0) = 0,$$
$$\frac{\partial T}{\partial y}(x,0) = -h_s T, \quad u(x,\infty) = U_\infty,\ T(x,\infty) = T_\infty \tag{4}$$

where, u and v are the x (along the plate) and the y (normal to the plate) component of velocities, respectively. U_∞ is the free stream velocity, λU_∞ is the plate velocity, where λ is the moving inclined plate parameter. Moreover, the $h_s = h_0 c x^{\frac{n-1}{2}}$ represents the heat transfer parameter for Newtonian heating, T is the temperature of the nanofluids, and σ is the electrical conductivity. The transverse magnetic field assumed to be a function of the distance from the origin is defined as $B(x) = B_0 x^{-\frac{1}{2}}$ with $B_0 \neq 0$, where x is the coordinate along the plate and B_0 is the magnetic field strength. The effective properties of nanofluids may be expressed in terms of the properties of base fluids, nanoparticles, and the volume fraction of solid nanoparticles as follows (Khan et al., 2015).

$$\rho_{nf} = (1-\phi)\rho_f + \phi\rho_s, \quad \mu_{nf} = \frac{\mu_f}{(1-\phi)^{2.5}},$$
$$(\rho C_p)_{nf} = (1-\phi)(\rho C_p)_f + \phi(\rho C_p)_s, \quad (\rho\beta)_{nf} = (1-\phi)(\rho\beta)_f + \phi(\rho\beta)_s \tag{5}$$
$$\alpha_{nf} = \frac{k_{nf}}{(\rho C_p)_{nf}}, \quad \frac{k_{nf}}{k_f} = \frac{k_s + 2k_f - 2\phi(k_f - k_s)}{k_s + 2k_f + \phi(k_f - k_s)}$$

where, ρ_{nf} is the effective density, ϕ is the solid volume fraction, ρ_f and ρ_s are the densities of pure fluid and nanoparticles, respectively. Moreover, μ_f is the dynamic viscosity of the base fluids, μ_{nf} is the effective dynamic viscosity, $(\rho C_p)_{nf}$ is the heat capacity of the nanofluids, $(\rho C_p)_f$ is specific heat parameters of the base fluids, $(\rho C_p)_s$ is the specific heat parameters of nanoparticles, $(\rho\beta)_{nf}$ is the thermal expansion coefficient, α_{nf} is the thermal diffusivity of the nanofluids, k_{nf} is the thermal conductivity of the nanofluids, k_f and k_s are thermal conductivities of the nanofluids and nanoparticles, respectively.

The continuity in Eq. 1 is satisfied by introducing a stream function $\psi(x, y)$ such as:

$$u = \frac{\partial\psi}{\partial y}, v = -\frac{\partial\psi}{\partial x} \tag{6}$$

The following similarity variables are introduced:

$$\eta = y\sqrt{\frac{U_\infty}{v_f x}} = \frac{y}{x}\sqrt{Re_x},\ \psi = v_f\sqrt{Re_x}f(\eta), \qquad \theta = \frac{T-T_\infty}{T_\infty} \quad (7)$$

where, η is the similarity variable, $Re_x = U_\infty x/v_f$ is the Reynolds number, $f(\eta)$ the non-dimensional stream function and $\theta(\eta)$ the non-dimensional temperature.

By applying Eqs. 5 and 6, as well as Eqs. 7 and 2, and Eq. 3, we simplify these into a nonlinear system of ordinary differential equations:

$$f''' + (1-\phi)^{2.5}\left(1-\phi+\phi\left(\frac{\rho_s}{\rho_f}\right)\right)\frac{1}{2}ff'' + (1-\phi)^{2.5}M(1-f')\sin^2\alpha + (1-\phi)^{2.5}\left(1-\phi+\phi\left(\frac{(\rho\beta)_s}{(\rho\beta)_f}\right)\right)Gr_x\theta\cos\gamma = 0 \quad (8)$$

$$\left(\frac{k_{nf}}{k_f}\right)\theta'' + \frac{\Pr}{2}\left(1-\phi+\phi\frac{(\rho C_p)_s}{(\rho C_p)_f}\right)f\theta' = 0 \quad (9)$$

subjected to the boundary conditions in Eq. 4, which becomes:

$$f(0) = 0,\ f'(0) = \lambda,\ \theta'(0) = -\omega(\theta(0)+1)$$
$$f'(\eta) = 1,\ \theta(\eta) = 0,\ \text{as}\ \eta \to \infty \quad (10)$$

where, primes denote differentiation with respect to η , $\omega = h_s\sqrt{\frac{v_f x}{U_\infty}}$ is the Newtonian heating parameter, $M = \sigma {B_0}^2/\rho U_\infty$ is the magnetic parameter, $Gr_x = g\beta_f T_\infty x/{U_\infty}^2$ is the local Grashof number and $\Pr = (\mu C_p)_f/k_f$ is the Prantl number. Note that λ denotes the direction of motion of the plate with $\lambda = 0$ for the static plate, while $\lambda = 0.2$ and $\lambda = -0.2$ for the fourth and back motion of the plate, respectively. In order to have a true similarity solution, the parameter Gr_x must be constant and independent of x. This condition will be satisfied if the thermal expansion coefficient β_f proportional to x^{-1}. Hence, by assuming the work of Makinde (2011), $\beta_f = ax^{-1}$, where a is a constant but have the appropriate dimension. Substituting $\beta_f = ax^{-1}$ into the parameter Gr_x will result in $Gr = agT_\infty/{U_\infty}^2$. The quantities of engineering interest are the skin-friction coefficient, C_f at the surface of the plate and the local Nusselt number, Nu_x, which is defined as:

$$C_f = \frac{\tau_w}{\rho_f {U_\infty}^2},\quad Nu_x = \frac{xq_w}{k_f(T-T_\infty)} \quad (11)$$

where, τ_w is the wall skin friction or shear stress at the plate and q_w is the heat flux from the plate, which is given by:

$$\tau_w = \mu_{nf}\left(\frac{\partial u}{\partial y}\right)_{y=0},\quad q_w = -k_{nf}\left(\frac{\partial T}{\partial y}\right)_{y=0} \quad (12)$$

Substituting Eqs. 7 and 12 into Eq. 11, we obtain:

$$(Re_x)^{\frac{1}{2}}C_f = \frac{1}{(1-\phi)^{2.5}}f''(0),\quad \frac{Nu_x}{(Re_x)^{\frac{1}{2}}} = -\frac{k_{nf}}{k_f}\frac{\theta'(0)}{\theta(0)} \quad (13)$$

3. Numerical solution

Eqs. 8 and 9, subject to the boundary conditions in Eq. 10 are solved numerically using the Keller-box method as described in the books of Na (1979) and Cebeci and Bradshaw (2012). The solution is achieved through four stages:

1. Transform Eqs. 8 and 9 into a first-order system.
2. Formulate the difference equations using central differences.
3. Use Newton's method to linearize the resulting algebraic equations and express them in matrix-vector format.
4. Apply the block tridiagonal elimination method to solve the linear system.

4. Result and discussion

In order to look into the physical insight of the problem, the velocity and temperature profiles against the dimensionless position η, for both magnetic nanofluids have been discussed by assigning different numerical values to the parameter: Angle for the aligned magnetic field α, magnetic strength M, angle of inclination of the plate γ, local Grashof number Gr_x, the volume fraction of nanoparticles ϕ and Newtonian heating parameter ω and their effects on flow and heat transfer characteristics are analyzed graphically.

Two different base fluids are considered, namely kerosene and water with magnetic nanoparticle Fe_3O_4. Table 1 shows the thermophysical properties of kerosene, water, and Fe_3O_4. The value of the Prandtl number for water is taken as 6.2, while 21 is the Prandtl number for kerosene. The effect of solid volume fraction ϕ is investigated in the range of $0 \leq \phi \leq 0.20$, in which $\phi = 0$ signifies pure fluid water or kerosene. To validate the numerical method's accuracy, a direct comparison was made with the previously reported numerical results of Blasius (1908) and Khan et al. (2015) for Fe_3O_4-water and Fe_3O_4-kerosene with respect to aligned magnetic field parameters in the absence of free convection parameter. From Table 2, the present results are observed to be in good agreement with those of the previous findings.

The variation in velocity and temperature profiles for different values of inclined angle of the magnetic field, α for magnetic nanofluids is disclosed in Fig. 2. As the values of α increase, velocity profiles gradually increase, but an increase in the inclined angle of the magnetic field α loses the motion of the fluid, which causes a reduction in the temperature of the fluid. When $\alpha = 0°$ it indicates that there is no magnetic field and because of the changes in the aligned field position of the magnetic field, it attracts the nanoparticles. It is noticed that a rise is detected in the momentum boundary layer while a decline is detected in the thermal boundary layer.

Table 1: Thermophysical properties of base fluids and nanoparticles (Mojumder et al., 2015; Sheikholeslami et al., 2015)

Physical properties	Water	Kerosene	Fe_3O_4
$\rho(kg/m^3)$	997.1	780	5200
$C_p(J/kgK)$	4179	2090	670
$k(W/mK)$	0.613	0.149	6
$\beta \times 10^{-5}(K^{-1})$	21	99	1.3
Pr	6.2	21	

Table 2: Comparison of the skin friction coefficient for different values of volume fraction of nanoparticles

	Volume friction	Skin friction $Gr_x = 0, \alpha = 90^o, \gamma = 0^o, M = 0$		
		Blasius (1908)	Khan et al. (2015)	Current study
Pure water	0	0.3321	0.33206	0.332059
Fe_3O_4-water	0.01	-	0.34324	0.343271
	0.05	-	-	0.389577
	0.10	-	0.45131	0.451635
	0.15	-	-	0.519813
	0.20	-	0.59517	0.595192
Pure kerosene	0	-	-	0.332059
Fe_3O_4-kerosene	0.01	-	0.34557	0.345611
	0.05	-	-	0.400879
	0.10	-	0.47336	0.473745
	0.15	-	-	0.552809
	0.20	-	0.63950	0.640265

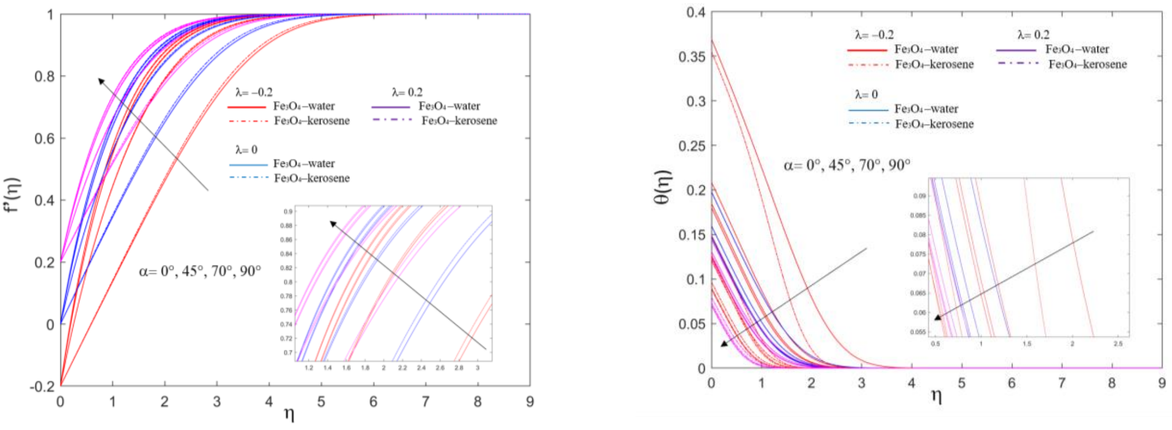

Fig. 2: Effect of aligned magnetic field parameters on the (a) velocity and (b) temperature profiles for M = 1, γ = 45°, Gr_x = 0.1, φ = 0.05, and ω = 0.1

The effects of different values of the magnetic strength, $M = 0, 1, 2,$ and 4 of the dimensionless velocity and temperature profiles are presented in Fig. 3. From Figs. 3a and 3b, the velocity increases while the temperature decreases as the values of M increase. These results are similar to those reported by Bosli et al. (2023) and Ilias et al. (2020). From Figs. 3a and 3b indicated that Fe_3O_4-kerosene shows the highest velocity profiles and lowest temperature compared to Fe_3O_4-water. However, based on Table 3, the skin friction, which measures the drag exerted by a moving fluid on the plate surface, also increases. This is due to the fact that Newtonian heating at the plate surface causes a high surface temperature, which results in an increase in the buoyancy force. When $M = 0$, this indicates that there is no magnetic force. It is means by when magnetic field value increase, it pushes the fluid towards the plate and thus, the momentum boundary layer decreases. This situation leads to an increase in magnetic nanofluids' velocity near the plate surface by overplaying the effect of the Lorentz force. Fig. 4a shows the effect of the angle of inclination γ on velocity profile for both magnetic nanofluids. The velocity decreases for increasing values of the angle of inclination γ. The fluid velocity is higher when the surface is vertical, $\gamma = 0°$ than when it is inclined. This is because the angle of inclination decreases the effect of the buoyancy force due to the gravity component. It is obvious that the buoyancy force is maximum for $\gamma = 0°$ and there is no buoyancy force for $\gamma = 90°$, horizontal plate. The temperature profile can be noticed in Fig. 4b. It is directly proportional to the increase in inclination angle. As γ increases, the skin friction decreases slightly while the temperature of magnetic nanofluids increases considerably. The momentum boundary layer and thermal boundary layer thickness become thicker with the increasing inclination angle.

The effects of the Grashof number Gr_x on velocity and temperature profiles are presented in Fig. 5. The velocity increases as the Grashof number increases. This is due to the presence of the buoyancy effect, which enhances the velocity. Since the Gr_x is the ratio of the buoyant to the viscous force that acts on a fluid. Rising buoyancy forces allow viscosity to decrease, and with it, the boundary layer of momentum decreases continuously. On the other hand, the increasing Grashof number reduced the temperature profile for both magnetic nanofluids.

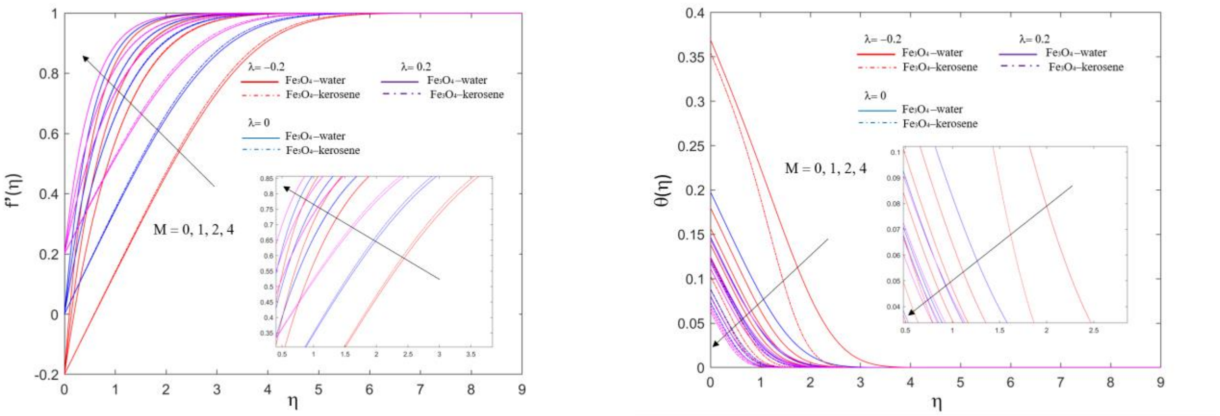

(a) (b)

Fig. 3: Effect of magnetic strength parameters on the (a) velocity and (b)temperature profiles for α = 90°, γ = 45°, Gr_x = 0.1, φ = 0.05, and ω = 0.1

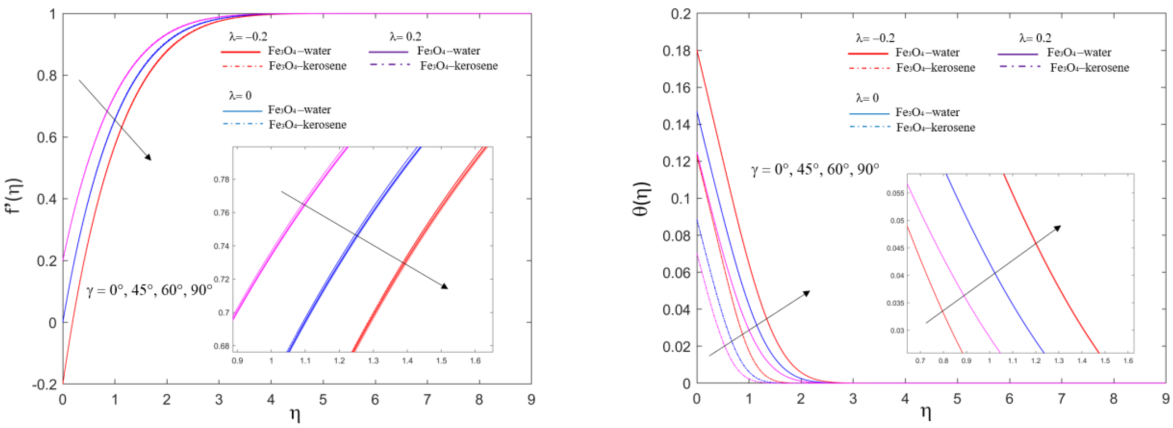

(a) (b)

Fig. 4: Effect of inclined plate parameters on the (a) velocity and (b) temperature profiles for α = 90°, M = 1, Gr_x = 0.1, ϕ = 0.05, and ω=0.1

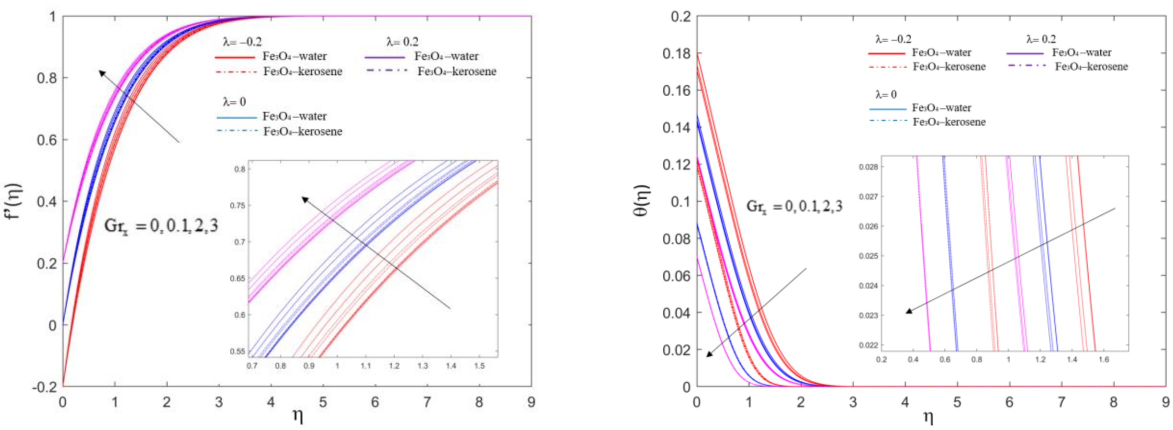

(a) (b)

Fig. 5: Effect of local Grashof number on the (a) velocity and (b) temperature profiles for α = 90°, M = 1, γ = 45°, ϕ = 0.05, and ω = 0.1

The dimensionless velocity for both magnetic nanofluids for different values of nanoparticle volume fraction is shown in Fig. 6. The velocity gets decelerated with increasing values of nanoparticles, but a converse action has been seen in the temperature profile. Increasing the volume fraction parameter results in an intensification of the temperature profile, in which the friction force is increased within the fluid. Therefore, it can be concluded that the temperature can be controlled by varying the nanoparticles' volume fraction as the temperature profile is higher for $\phi = 0.20$. The enhancement of magnetic nanofluids' thermal conductivity is linked to the delicacy of the width of the thermal boundary layer by ϕ. To put it another way, the higher the thermal conductivity of a fluid, the higher the thermal diffusivity.

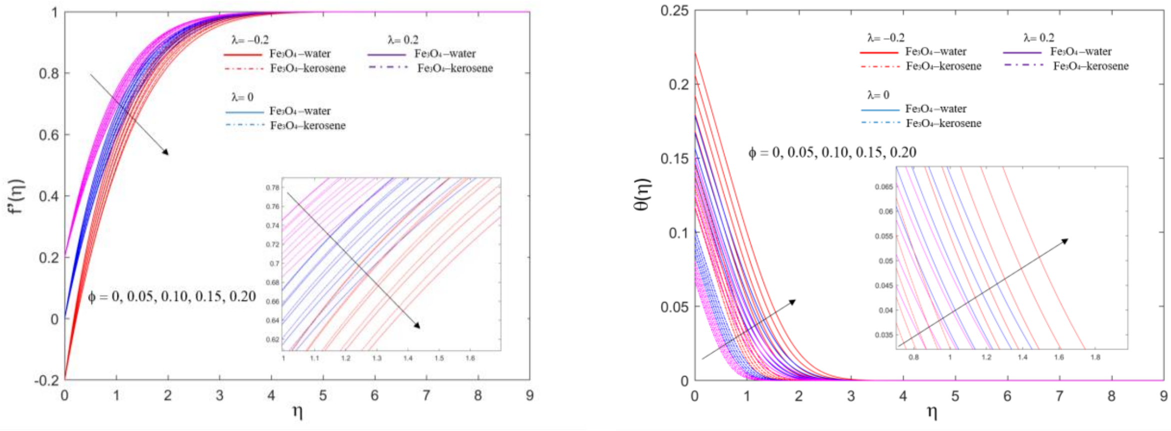

(a) (b)

Fig. 6: Effect of volume fraction of nanoparticles on the (a) velocity and (b) temperature profiles for α = 90°, M = 1, γ = 45°, Gr_x = 0.1, and ω = 0.1

It is observed that an increase in the Newtonian heating parameter, ω, boosts the velocity profile as well as momentum boundary layer thickness (Fig. 7a). The behaviour of ω on temperature profile is analyzed in Fig. 7b. Obviously, temperature and thermal boundary layer tend to decrease for a rise in Newtonian heating parameter. Newtonian heating expresses that the heat-transfer rate through a sidewall is proportional to the local sidewall temperature.

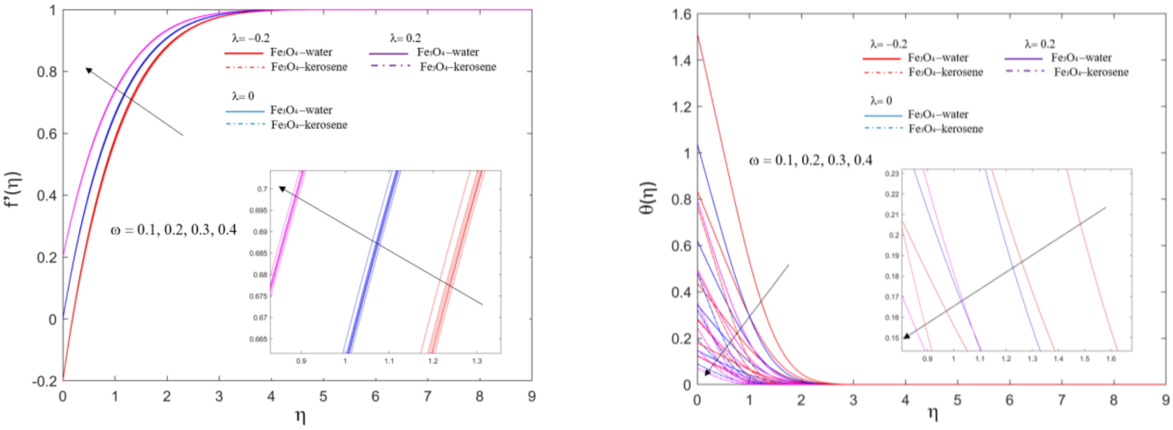

(a) (b)

Fig. 7: Effect of Newtonian heating parameter on the (a) velocity and (b) temperature profiles for α = 90°, M = 1, γ = 45°, Gr_x = 0.1, and ϕ = 0.05

Based on Table 3 and Table 4, it was clearly stated the skin friction coefficient at the wall of the inclined plate is increasing in magnitude with an increase in aligned magnetic field α, magnetic strength M, Grashof number Gr_x, the volume fraction of nanoparticles ϕ, for both magnetic nanofluids and Newtonian heating parameters ω. The highest wall shear stress occurs when the magnetic strength of the moving inclined plate against the flow, $\lambda = -0.2$ increases. The increasing pattern for Nusselt number occurs for the same parameters of skin friction, and the highest rate of heat transfer occurs when the volume fraction of nanoparticles increases for moving inclined plate along the flow, $\lambda = 0.2$ for both Fe_3O_4-water and Fe_3O_4-kerosene.

5. Conclusion

Physically, aligned magnetic field parameter α, magnetic strength parameter M, the inclination of plate parameter γ, Grashof number Gr_x, the volume fraction of nanoparticles ϕ and Newtonian heating parameter ω were studied in detail, and the results are discussed graphically.

From the results and discussion, the following specific conclusions for both magnetic nanofluids are obtained:

- The velocity of both magnetic nanofluids increases due to increasing α, M, Gr_x and ω.
- The velocity of both magnetic nanofluids decreases with the increase in γ and ϕ.
- The temperature of magnetic nanofluids decreases when the parameter of $\alpha, M, Gr_x,$ and ω are increasing.
- The temperature of magnetic nanofluids increases with the increase in γ and ϕ.
- The skin friction coefficient increases due to increasing α, M, Gr_x, ϕ and ω.
- The skin friction coefficient decreases due to increasing γ.

- The Nusselt number gets enhanced due to an increase in α, M, Gr_x, ϕ and ω.
- The Nusselt number decreases when γ increases.
- The velocity of both magnetic nanofluids increases faster for moving the inclined plate along the flow compared to moving the inclined plate against the flow due to an increase in M.
- The temperature of both magnetic nanofluids decreased faster for moving the inclined plate along the flow compared to moving the inclined plate against the flow due to an increase in M.

Table 3: Variation in skin friction coefficient and Nusselt number at different dimensionless parameters for Fe_3O_4-water

α	M	γ	Gr_x	ϕ	ω	Fe_3O_4-water					
						Skin friction			Nusselt number		
						$\lambda=-0.2$	$\lambda=0$	$\lambda=0.2$	$\lambda=-0.2$	$\lambda=0$	$\lambda=0.2$
0°						0.390526	0.401097	0.374142	0.413811	0.675797	0.884818
45°	1	45°	0.1	0.05	0.1	0.974740	0.842653	0.698469	0.646475	0.810865	0.964048
70°						1.253845	1.068085	0.873224	0.715651	0.859877	0.997307
90°						1.327643	1.128218	0.920244	0.731533	0.871496	1.005430
	0					0.390526	0.401097	0.374142	0.413811	0.675797	0.884818
90°	1	45°	0.1	0.05	0.1	1.327643	1.128218	0.920244	0.731533	0.871496	1.005430
	2					1.842597	1.551014	1.253387	0.823089	0.940569	1.055194
	3					2.581939	2.162619	1.739019	0.916707	1.014019	1.110244
		0°				1.330294	1.130201	0.921801	0.732065	0.871842	1.005665
90°	1	45°	0.1	0.05	0.1	1.327643	1.128218	0.920244	0.731533	0.871496	1.005430
		60°				1.325764	1.126814	0.919143	0.731156	0.871251	1.005262
		90°				1.321214	1.123420	0.916481	0.730241	0.870659	1.004859
			0			1.321214	1.123420	0.916481	0.730241	0.870659	1.004859
90°	1	45°	0.1	0.05	0.1	1.327643	1.128218	0.920244	0.731533	0.871496	1.005430
			2			1.443176	1.216506	0.990345	0.754149	0.886633	1.015938
			3			1.499742	1.260994	1.026239	0.764831	0.894076	1.021229
				0		1.237918	1.048399	0.852391	0.693366	0.825912	0.953219
				0.05		1.327643	1.128218	0.920244	0.731533	0.871496	1.005430
90°	1	45°	0.1	0.10	0.1	1.428831	1.218274	0.996807	0.768839	0.916723	1.057703
				0.15		1.543682	1.320526	1.083741	0.805206	0.961609	1.110141
				0.20		1.674988	1.437462	1.183160	0.840512	1.006141	1.162830
					0.1	1.327643	1.128218	0.920244	0.731533	0.871496	1.005430
90°	1	45°	0.1	0.05	0.2	1.336817	1.134641	0.925069	0.733371	0.872614	1.006161
					0.3	1.350900	1.143663	0.931474	0.736177	0.874180	1.007129
					0.4	1.374967	1.157212	0.940373	0.740933	0.876522	1.008471

Table 4: Variation of skin friction coefficient and Nusselt number at different dimensionless parameters for Fe_3O_4-kerosene

α	M	γ	Gr_x	ϕ	ω	Fe_3O_4-kerosene					
						Skin friction			Nusselt number		
						$\lambda=-0.2$	$\lambda=0$	$\lambda=0.2$	$\lambda=-0.2$	$\lambda=0$	$\lambda=0.2$
0°						0.394100	0.405806	0.380720	0.437261	1.064942	1.552865
45°	1	45°	0.1	0.05	0.1	0.974460	0.844177	0.701071	0.883899	1.300338	1.676167
70°						1.253463	1.069035	0.874977	1.017912	1.387825	1.730531
90°						1.327248	1.129064	0.921836	1.048754	1.408776	1.744046
	0					0.394100	0.405806	0.380720	0.437261	1.064942	1.552865
90°	1	45°	0.1	0.05	0.1	1.327248	1.129064	0.921836	1.048754	1.408776	1.744046
	2					1.842195	1.551431	1.254283	1.227722	1.535320	1.829001
	4					2.581597	2.162816	1.739513	1.414334	1.674562	1.927734
		0°				1.328657	1.129930	0.922436	1.049241	1.409014	1.744177
90°	1	45°	0.1	0.05	0.1	1.327248	1.129064	0.921836	1.048754	1.408776	1.744046
		60°				1.326251	1.128452	0.921412	1.048409	1.408608	1.743953
		90°				1.323837	1.126973	0.920388	1.047574	1.408201	1.743728
			0			1.323837	1.126973	0.920388	1.047574	1.408201	1.743728
90°	1	45°	0.1	0.05	0.1	1.327248	1.129064	0.921836	1.048754	1.408776	1.744046
			2			1.389741	1.168230	0.949173	1.070048	1.419457	1.750009
			3			1.421058	1.188434	0.963423	1.080493	1.424906	1.753099
				0		1.235277	1.046005	0.850331	0.958385	1.282046	1.584835
				0.05		1.327248	1.129064	0.921836	1.048754	1.408776	1.744046
90°	1	45°	0.1	0.10	0.1	1.431046	1.222857	1.002577	1.140235	1.539845	1.910240
				0.15		1.548917	1.329411	1.094290	1.232662	1.675588	2.084169
				0.20		1.683723	1.451312	1.199191	1.325793	1.816371	2.266704
					0.1	1.327248	1.129064	0.921836	1.048754	1.408776	1.744046
90°	1	45°	0.1	0.05	0.2	1.331592	1.131558	0.923502	1.050255	1.409461	1.744411
					0.3	1.337304	1.134580	0.925440	1.052223	1.410290	1.744834
					0.4	1.345131	1.138319	0.927719	1.054911	1.411314	1.745333

List of symbols

α	Aligned angle of magnetic field
α_{nf}	Thermal diffusivity of magnetic nanofluids
β_f	Thermal expansion coefficient
γ	Plate inclination angle
η	Boundary layer thickness
$\theta(\eta)$	Non – dimensional temperature function
λ	Velocity ratio parameter
μ_f	Dynamic viscosity of base fluid
μ_{nf}	Dynamic viscosity of magnetic nanofluids
ρ	Density
ρ_f	Density of base fluid
ρ_s	Density of nanoparticles
ρ_{nf}	Density of magnetic nanofluids
$(\rho C_p)_{nf}$	Heat capacity of magnetic nanofluids
$(\rho C_p)_f$	Heat parameters of base fluid
$(\rho C_p)_s$	Heat parameters of nanoparticles
$(\rho\beta)_{nf}$	Thermal expansion of magnetic nanofluids coefficient
σ	Electrical conductivity
τ_w	Wall shear stress
ϕ	Nanoparticles volume fraction
$\psi(x,y)$	Stream function
$B(x)$	Transverse magnetic field
B_0	Magnetic field strength

Bi_x	Biot number
$f(\eta)$	Non – dimensional stream function
C_f	Local skin – friction coefficient
Gr_x	Local Grashof number
g	Gravitational acceleration
h_f	Heat transfer coefficient
k_f	Thermal conductivity of base fluid
k_s	Thermal conductivity of nanoparticles.
k_{nf}	Thermal conductivity of magnetic nanofluids
M	Magnetic strength parameter
Nu_x	Local Nusselt number
Pr	Prantl number
q_w	Heat flux
Re_x	Reynolds number
T	Temperature
T_f	Temperature of hot fluid
T_∞	Temperature at the free stream
$U_w(x)$	Plate velocity
U_∞	Velocity in free stream
u	Velocity in x-direction
v	Velocity in y-direction
x	Dimensionless coordinate axis along the inclined plate
y	Dimensionless coordinate axis normal to the surface plate

Acknowledgment

The authors extend their appreciation to Universiti Teknologi MARA Cawangan Kedah for funding this work through Geran Dana Kecemerlangan under grant number 600-UiTMKDH (PJI.5/4/1) (9/2018).

Compliance with ethical standards

Conflict of interest

The author(s) declared no potential conflicts of interest with respect to the research, authorship, and/or publication of this article.

References

Ahmad SZAS, Hamzah WAW, Ilias MR, Shafie S, and Najafi G (2019). Unsteady MHD boundary layer flow and heat transfer of ferrofluids over a horizontal flat plate with leading edge accretion. Journal of Advanced Research in Fluid Mechanics and Thermal Sciences, 59(2): 163-181.

Aleem M, Asjad MI, Shaheen A, and Khan I (2020). MHD influence on different water based nanofluids (TiO_2, Al_2O_3, CuO) in porous medium with chemical reaction and Newtonian heating. Chaos, Solitons and Fractals, 130: 109437. https://doi.org/10.1016/j.chaos.2019.109437

Arulmurugan R, Vaidyanathan G, Sendhilnathan S, and Jeyadevan B (2006). Mn–Zn ferrite nanoparticles for ferrofluid preparation: Study on thermal–magnetic properties. Journal of Magnetism and Magnetic Materials, 298(2): 83-94. https://doi.org/10.1016/j.jmmm.2005.03.002

Blasius H (1908). Grenzschichten in flüssigkeiten mit kleiner reibung. Zeitschrift für Angewandte Mathematik und Physik, 56: 1-37.

Blums E (2002). Heat and mass transfer phenomena. In: Odenbach S (Ed.), Ferrofluids: Magnetically controllable fluids and their applications: 124-139. Springer Berlin Heidelberg, Berlin, Germany. https://doi.org/10.1007/3-540-45646-5_7

Bosli F, Ilias MR, Aznam NHZ, Ishak SS, Zakaria SF, and Rahim AHA (2023). Aligned magnetohydrodynamic effect on magnetic nanoparticle with different base fluids past a moving inclined plate. International Journal of Advanced and Applied Sciences 10(3): 96-107. https://doi.org/10.21833/ijaas.2023.03.013

Bosli F, Suhaimi AS, Ishak SS, Ilias MR, Rahim AHA, and Ahmad AM (2022). Investigation of nanoparticles shape effects on aligned MHD Casson Nanofluid flow and heat transfer with convective boundary condition. Journal of Advanced Research in Fluid Mechanics and Thermal Sciences, 91(1): 155-171. https://doi.org/10.37934/arfmts.91.1.155171

Bozhko AA and Putin GF (2003). Heat transfer and flow patterns in ferrofluid convection. Magnetohydrodynamics, 39(2): 147-169. https://doi.org/10.22364/mhd.39.2.2

Cebeci T and Bradshaw P (2012). Physical and computational aspects of convective heat transfer. Springer Science and Business Media, Berlin, Germany.

Choi SU and Eastman JA (1995). Enhancing thermal conductivity of fluids with nanoparticles (No. ANL/MSD/CP-84938; CONF-951135-29). Argonne National Lab (ANL), Argonne, USA.

Ganguly R, Sen S, and Puri IK (2004). Heat transfer augmentation using a magnetic fluid under the influence of a line dipole. Journal of Magnetism and Magnetic Materials, 271(1): 63-73. https://doi.org/10.1016/j.jmmm.2003.09.015

Hamdan FR, Kamal MHA, Rawi NA, Mohamad AQ, Ali A, Ilias MR, and Shafie S (2020). G-jitter free convection flow near a three-dimensional stagnation-point region with internal heat generation. Journal of Advanced Research in Fluid Mechanics and Thermal Sciences, 67(1): 119-135.

Hayat T, Khan MI, Waqas M, and Alsaedi A (2017). Newtonian heating effect in nanofluid flow by a permeable cylinder. Results in Physics, 7: 256-262. https://doi.org/10.1016/j.rinp.2016.11.047

Ilias MR (2018). Steady and unsteady aligned magnetohydrodynamics free convection flows of magnetic and non magnetic nanofluids along a wedge, vertical and inclined plates. Ph.D. Dissertation, Universiti Teknologi Malaysia, Johor Bahru, Malaysia.

Ilias MR, Ismail NSA, AbRaji NH, Rawi NA, and Shafie S (2020). Unsteady aligned MHD boundary layer flow and heat transfer of a magnetic nanofluids past an inclined plate. International Journal of Mechanical Engineering and Robotics Research, 9(2): 197-206. https://doi.org/10.18178/ijmerr.9.2.197-206

Ilias MR, Rawi NA, and Shafie S (2016). MHD free convection flow and heat transfer of ferrofluids over a vertical flat plate with aligned and transverse magnetic field. Indian Journal of Science and Technology, 9(36): 1-7. https://doi.org/10.17485/ijst/2016/v9i36/97347

Ilias MR, Rawi NA, and Shafie S (2017a). Natural convection of ferrofluid from a fixed vertical plate with aligned magnetic field and convective boundary condition. Malaysian Journal of Fundamental and Applied Sciences, 13(3): 223-228. https://doi.org/10.11113/mjfas.v13n3.651

Ilias MR, Rawi NA, and Shafie S (2017b). Steady aligned MHD free convection of Ferrofluids flow over an inclined plate. Journal of Mechanical Engineering, 14(2): 1-15.

Ilias MR, S'aidah IN, Esah WS, and Hussain C (2018). Unsteady aligned MHD boundary layer flow of a magnetic nanofluid over a wedge. International Journal of Civil Engineering and Technology, 9: 794-810.

Ishak SS, Mazlan NN, Ilias MR, Osman R, Kasim ARM, and Mohammad NF (2022). Radiation effects on inclined magnetohydrodynamics mixed convection boundary layer flow of hybrid nanofluids over a moving and static wedge. Journal of Advanced Research in Applied Sciences and Engineering Technology, 28(3): 68-84. https://doi.org/10.37934/araset.28.3.6884

Jue TC (2006). Analysis of combined thermal and magnetic convection ferrofluid flow in a cavity. International

Communications in Heat and Mass Transfer, 33(7): 846-852. https://doi.org/10.1016/j.icheatmasstransfer.2006.02.001

Khan WA, Khan ZH, and Haq RU (2015). Flow and heat transfer of ferrofluids over a flat plate with uniform heat flux. The European Physical Journal Plus, 130: 86. https://doi.org/10.1140/epjp/i2015-15086-4

Khashi'ie NS, Arifin NM, Hafidzuddin EH, Wahi N, and Ilias MR (2019). Magnetohydrodynamics (MHD) flow and heat transfer of a doubly stratified nanofluid using Cattaneo-Christov model. Universal Journal of Mechanical Engineering, 7(4): 206-214. https://doi.org/10.13189/ujme.2019.070409

Lajvardi M, Moghimi-Rad J, Hadi I, Gavili A, Isfahani TD, Zabihi F, and Sabbaghzadeh J (2010). Experimental investigation for enhanced ferrofluid heat transfer under magnetic field effect. Journal of Magnetism and Magnetic Materials, 322(21): 3508-3513. https://doi.org/10.1016/j.jmmm.2010.06.054

Makinde OD (2011). Similarity solution for natural convection from a moving vertical plate with internal heat generation and a convective boundary condition. Thermal Science, 15(Suppl. 1): S137-S143. https://doi.org/10.2298/TSCI11S1137M

Makinde OD (2013). Effects of viscous dissipation and Newtonian heating on boundary-layer flow of nanofluids over a flat plate. International Journal of Numerical Methods for Heat and Fluid Flow, 23(8): 1291-1303. https://doi.org/10.1108/HFF-12-2011-0258

Merkin JH (1994). Natural-convection boundary-layer flow on a vertical surface with Newtonian heating. International Journal of Heat and Fluid Flow, 15(5): 392-398. https://doi.org/10.1016/0142-727X(94)90053-1

Mohamad AQ, Noranuar WNIN, Isa ZM, Shafie S, Kasim ARM, Illias MR, and Jiann LY (2022). Natural convection flow of Casson fluid with carbon nanotubes past an accelerated disk. In the International Conference on Mathematical Sciences and Statistics 2022, Atlantis Press, Wuhan, China: 484-497. https://doi.org/10.2991/978-94-6463-014-5_41

Mohamed MKA, Ismail NA, Hashim N, Shah NM, and Salleh MZ (2019). MHD slip flow and heat transfer on stagnation point of a magnetite (Fe_3O_4) ferrofluid towards a stretching sheet with Newtonian heating. CFD Letters, 11(1): 17-27.

Mojumder S, Saha S, Saha S, and Mamun MAH (2015). Effect of magnetic field on natural convection in a C-shaped cavity filled with ferrofluid. Procedia Engineering, 105: 96-104. https://doi.org/10.1016/j.proeng.2015.05.012

Na TY (1979). Computational methods in engineering boundary value problems. Academic Press, New York, USA.

Nayan A, Fauzan NIFA, Ilias MR, Zakaria SF, and Aznam NHZ (2022). Aligned magnetohydrodynamics (MHD) flow of hybrid nanofluid over a vertical plate through porous medium. Journal of Advanced Research in Fluid Mechanics and Thermal Sciences, 92(1): 51-64. https://doi.org/10.37934/arfmts.92.1.5164

Noranuar WNIN, Mohamad AQ, Shafie S, Khan I, Jiann LY, and Ilias MR (2021). Non-coaxial rotation flow of MHD Casson nanofluid carbon nanotubes past a moving disk with porosity effect. Ain Shams Engineering Journal, 12(4): 4099-4110. https://doi.org/10.1016/j.asej.2021.03.011

Prasher R, Song D, Wang J, and Phelan P (2006). Measurements of nanofluid viscosity and its implications for thermal applications. Applied Physics Letters, 89(13): 133108. https://doi.org/10.1063/1.2356113

Reddy PS and Sreedevi P (2021). Effect of thermal radiation and volume fraction on carbon nanotubes based nanofluid flow inside a square chamber. Alexandria Engineering Journal, 60(1): 1807-1817. https://doi.org/10.1016/j.aej.2020.11.029

Rosaidi NA, Ab Raji NH, Ibrahim SNHA, and Ilias MR (2022). Aligned magnetohydrodynamics free convection flow of magnetic nanofluid over a moving vertical plate with convective boundary condition. Journal of Advanced Research in Fluid Mechanics and Thermal Sciences, 93(2): 37-49. https://doi.org/10.37934/arfmts.93.2.3749

Sheikholeslami M and Rashidi MM (2015). Ferrofluid heat transfer treatment in the presence of variable magnetic field. The European Physical Journal Plus, 130: 115. https://doi.org/10.1140/epjp/i2015-15115-4

Sheikholeslami M, Ganji DD, and Rashidi MM (2015). Ferrofluid flow and heat transfer in a semi annulus enclosure in the presence of magnetic source considering thermal radiation. Journal of the Taiwan Institute of Chemical Engineers, 47: 6-17. https://doi.org/10.1016/j.jtice.2014.09.026

Singh G and Makinde OD (2012). Computational dynamics of MHD free convection flow along an inclined plate with Newtonian heating in the presence of volumetric heat generation. Chemical Engineering Communications, 199(9): 1144-1154. https://doi.org/10.1080/00986445.2011.651184

Soid SK, Durahman AA, Norzawary NHA, Ilias MR, and Sahar AM (2022). Magnetohydrodynamic of copper-aluminium of oxide hybrid nanoparticles containing gyrotactic microorganisms over a vertical cylinder with suction. Journal of Advanced Research in Applied Sciences and Engineering Technology, 28(2): 222-234. https://doi.org/10.37934/araset.28.2.222234

Sreedevi P, Reddy PS, and Suryanarayana Rao KV (2021). Effect of magnetic field and radiation on heat transfer analysis of nanofluid inside a square cavity filled with silver nanoparticles: Tiwari–Das model. Waves in Random and Complex Media. https://doi.org/10.1080/17455030.2021.1918798

Tiwari RK and Das MK (2007). Heat transfer augmentation in a two-sided lid-driven differentially heated square cavity utilizing nanofluids. International Journal of Heat and Mass Transfer, 50(9-10): 2002-2018. https://doi.org/10.1016/j.ijheatmasstransfer.2006.09.034

Uddin MJ, Khan WA, and Ismail AI (2012). MHD free convective boundary layer flow of a nanofluid past a flat vertical plate with Newtonian heating boundary condition. PLOS ONE, 7(11): e49499. https://doi.org/10.1371/journal.pone.0049499 **PMid:23166688 PMCid:PMC3499543**

Ullah I, Shafie S, and Khan I (2017). Effects of slip condition and Newtonian heating on MHD flow of Casson fluid over a nonlinearly stretching sheet saturated in a porous medium. Journal of King Saud University-Science, 29(2): 250-259. https://doi.org/10.1016/j.jksus.2016.05.003

Wen D and Ding Y (2004). Experimental investigation into convective heat transfer of nanofluids at the entrance region under laminar flow conditions. International Journal of Heat and Mass Transfer, 47(24): 5181-5188. https://doi.org/10.1016/j.ijheatmasstransfer.2004.07.012

Xuan Y and Li Q (2000). Heat transfer enhancement of nanofluids. International Journal of Heat and Fluid Flow, 21(1): 58-64. https://doi.org/10.1016/S0142-727X(99)00067-3

Yasin SHM, Mohamed MKA, Ismail Z, Widodo B, and Salleh MZ (2019). Numerical solution on MHD stagnation point flow in ferrofluid with Newtonian heating and thermal radiation effect. Journal of Advanced Research in Fluid Mechanics and Thermal Sciences, 57(1): 12-22.

Yu W, France DM, Routbort JL, and Choi SU (2008). Review and comparison of nanofluid thermal conductivity and heat transfer enhancements. Heat Transfer Engineering, 29(5): 432-460. https://doi.org/10.1080/01457630701850851